Interannual Variability of the Australian Summer Monsoon Onset: Possible Influence of Indian Summer Monsoon and El Niño

PORATHUR V. JOSEPH AND BRANT LIEBMANN

Cooperative Institute for Research in Environmental Sciences, University of Colorado, Boulder, Colorado

HARRY H. HENDON

Center for Atmospheric Theory and Analysis, University of Colorado, Boulder, Colorado

(Manuscript received 9 May 1990, in final form 16 October 1990)

ABSTRACT

The date of Australian summer monsoon onset (ASMO) is found to be well correlated with the monsoon rainfall of India during the preceding June to September. Years of below (above) normal Indian summer monsoon rainfall (ISMR) are followed by delayed (early) ASMO. Sea surface temperature (SST) anomalies during the September to November season over the tropical Indian Ocean, the equatorial eastern Pacific Ocean, and the ocean north of Australia also correlate significantly with the date of the following ASMO. Delays in ASMO are associated with cold SST north of Australia and warm SST in the tropical Indian and equatorial east Pacific oceans.

Previous studies have shown that a warm SST is created over the tropical Indian Ocean in years of poor ISMR. We hypothesize that a warm SST anomaly over the Indian Ocean delays the seasonal southward and eastward migration of the cloudiness maximum. A delay in the southeastward movement of cloudiness results in a delayed ASMO. A similar hypothesis already has been suggested to explain the variability of the date of monsoon onset over India.

Weak ISMR often is associated with the contemporaneous presence of El Niño, although many weak monsoons occur without El Niño. Thus warm SSTs in the eastern equatorial Pacific are related to a delayed ASMO through the Indian monsoon. Another signature of El Niño is the presence of negative SST anomalies north of Australia, adding to the delay in ASMO. Warm SSTs in the central and eastern Pacific may also act directly to delay ASMO by causing convection near and east of the date line and subsidence near Australia.

1. Introduction

Onset of the Australian summer monsoon is marked by a sudden transition from a dry to a wet regime over northern Australia (e.g., Davidson et al. 1983). Large-scale circulation changes accompany onset (Troup 1961; Davidson et al. 1983; Murakami et al. 1986; Hendon and Liebmann 1990). Since the date of onset exhibits large interannual variability (Nicholls 1984a; Holland 1986; Hendon and Liebmann 1990), an advance knowledge of the approximate date of onset would be useful.

Prediction of the Australian Summer Monsoon Onset (ASMO) date is possible with some degree of success based on antecedent sea level pressure at Darwin (Nicholls and Woodcock 1981; Nicholls et al. 1982; Nicholls 1984a) and sea surface temperature (SST) in the eastern Pacific (Holland 1986). In the present paper we present evidence for an association between the strength of the Indian summer monsoon and the date of ASMO that follows and also a physical basis regarding the cause of ASMO variability.

Corresponding author address: Dr. Porathur V. Joseph, CIRES, University of Colorado, Campus Box 449, Boulder, CO 80309-0449.

2. Data and methodology

ASMO is characterized by a large-scale reversal of low-level winds to westerly and upper-level winds to easterly and a rapid increase of rainfall over northern Australia (Troup 1961; Nicholls et al. 1982; Nicholls 1984a; Holland 1986; Hendon and Liebmann 1990). Typically, the Australian monsoon consists of 2–3 cycles of heavy rainfall, each lasting more than 10 days, followed by a somewhat longer break. The average period from peak-to-peak activity is around 40 days (Holland 1986). Hendon and Liebmann (1990) concluded that onset of the Australian monsoon in most years is a manifestation of the 40- to 50-day oscillation as the seasonal cycle of convection and the 40- to 50-day activity moves south of the equator during the Southern Hemisphere warm season (Murakami et al. 1986; Gutzler and Madden 1989).

ASMO has been defined in various ways. Troup (1961) defined it as the first rainfall event after 1 No-

vember at six stations near Darwin. Davidson et al. (1983, 1984) used the first flareup of convective activity over northern Australia as determined by satellite.

Single station indices have been used successfully as well. Nicholls (1984a) defined onset at a number of stations over northern Australia as the date on which 15% of the mean annual rainfall has occurred. He deliberately chose a rainfall rather than a circulation index from a belief that users of long-range forecasts are more interested in rainfall than large-scale circulation changes.

Holland (1986) defined ASMO using an index of weakly low-pass filtered 850 mb wind at Darwin. Onset was considered to be the first occurrence of 850 mb westerlies. He rejected a rainfall-based definition because sporadic rainfall due to isolated thunderstorms can occur before any large-scale circulation changes. The correlation between Holland's index and that of Nicholls is only 0.49.

Most recently, Hendon and Liebmann (1990) used a combined wind and rainfall index to determine ASMO. Combining rainfall and wind should assure that a true change in the large-scale circulation has occurred. They defined onset as the first occurrence of 850-mb westerlies (lightly filtered to remove synoptic fluctuations) at Darwin that accompany an area-averaged rainfall over northern Australia of 7.5 mm day^{-1} (the climatological mean rainfall when winds turn westerly). The correlations between the Hendon and Liebmann index and indices of Nicholls (1984a) and Holland (1986) are 0.68 and 0.74, respectively. In the present study we use the onset dates as defined by Hendon and Liebmann for the 30 years from 1957/58 through 1986/87. Their mean date for ASMO is 25 December and its standard deviation is 16 days.

The ISMR data are taken from Mooley and Parthasarathy (1984a) for the period 1957 to 1978. Parthasarathy (personal communication) kindly provided the updated data for the period 1979 to 1986. ISMR is the area-weighted average rainfall of 306 fairly evenly spaced stations throughout India (excluding the mountainous region in the north) for each monsoon season (June, July, August, September). Mean ISMR for the period 1957–86 is 839 mm, and its standard deviation is 89 mm.

The SST data source is the COADS monthly mean summary trimmed file, in which SST is archived into 2° by 2° boxes. Observations of more than 3.5 standard deviations away from the median have been eliminated (Fletcher et al. 1983; Slutz et al. 1985; Woodruff et al. 1987). This method systematically underestimates the SST field during extremely anomalous periods (Wolter et al. 1989).

COADS data tapes contain SST anomalies calculated as seasonal departures from the 1950 to 1979 mean in each 2° by 2° box. They were averaged into 12° latitude by 24° longitude boxes, area weighted by a cosine correction applied to latitude. An 11-year running seasonal mean trend was removed from each box. Thus correlations involving SST are for the 27-year period 1957–83, unless otherwise specified.

Good data coverage exists from 1949 onwards. Figure 1 shows the average number of 2° by 2° boxes within each of the larger boxes that contain SST data during the September to November season from 1957 through 1983 (27 years). The maximum possible for a region fully over the sea is 72. There is more than 50% coverage in every box, except for a few in the southeast Pacific.

We also use outgoing longwave radiation (OLR) measurements obtained from NOAA operational satellites. In the tropics low values of OLR are indicative of convective cloudiness. Data are available from mid-1974 through 1988, not including most of 1978. The data were archived twice daily on a 2.5° grid.

3. Relation between ISMR and ASMO

Figure 2 is a scatter diagram between ISMR and the date of the following ASMO. The linear correlation coefficient between the two is −0.56, implying that a late ASMO should follow a weak ISMR. A two-sided t-test requires a correlation of 0.47 for significance at the 99% level after reducing the effective number of degrees of freedom due to serial correlation for lags 1 to 3 (Quenouille 1952); the actual correlation well ex-

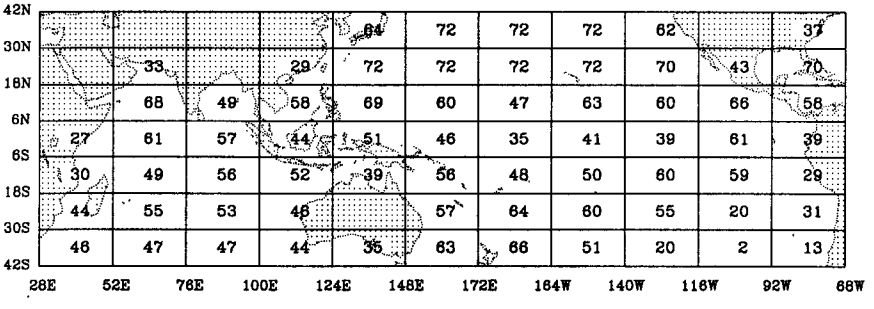

FIG. 1. Average number of 2° latitude–longitude squares containing monthly mean SST data in each 12° latitude × 24° longitude box in a SON season during 1957–1983. The maximum possible number for a box fully over the ocean is 72.

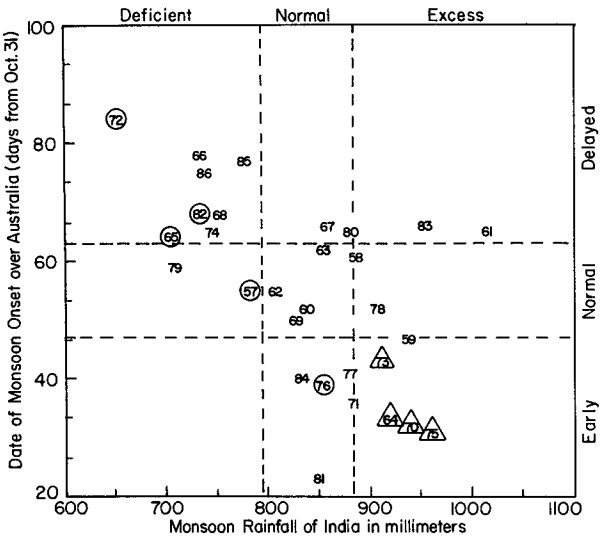

FIG. 2. Scatter diagram between June to September ISMR in millimeters for each of the 30 years 1957–1986 and the date of the following ASMO. ASMO counted as days from 31 October (i.e., 1 November is day 1). Last two digits of year of ISMR mark the location. Each axis is divided into categories of one-half standard deviation and more above the mean, normal, and one-half standard deviation and more below the mean. El Niño years are circled and cold event years are triangled.

ceeds that level. Both quantities on the scatter diagram are divided into three categories, a half standard deviation or more above the mean (excess ISMR, delayed ASMO), near normal, and a half standard deviation or more below the mean (deficient ISMR, early ASMO). Thus "normal" onset occurs between 18 December and 1 January (inclusive), and "normal" rainfall lies between 795 and 883 mm.

As we expect from the negative correlation, most years lie along the diagonal from upper left to lower right; early (delayed) ASMO follows excess (deficient) ISMR. The diagram shows that of the 30-year sample, 18 years lie within the expected categories. Furthermore, the opposite relationship, excess ISMR with delayed ASMO, occurs in only two years, 1961 and 1983.

Moderate to strong El Niño, or "warm" events (Quinn et al. 1987) and anti-El Niño, or "cold" events (Kiladis and Diaz 1989) are circled and triangled, respectively. A warm or cold event occurred in nine years of the 30-year sample. Of the ten years of deficient rainfall, four are associated with a warm event (one El Niño is associated with normal rainfall) and none with a cold event. Of the ten years of excess rainfall, four are associated with a cold event and none with a warm event. Thus, all of the cold events are associated with excess rainfall. The statistical association found previously between rainfall and El Niño (e.g., Rasmusson and Carpenter 1983) is apparent in the figure. It is also clear, however, that many cases of deficient (excess) rainfall are not associated with El Niño (cold) events.

Three of the five El Niños are associated with delayed onset (there are 12 cases of delayed onset) and one El Niño each with a normal and an early onset. All four of the cold events are associated with an early onset (there are 10 cases of early onset).

4. Relationship of anomalous SST to ISMR and ASMO

Figure 3 shows the correlation between (June–September) ISMR and SST anomalies during the following September, October, November (SON) season. A two-sided *t*-test (not corrected for serial correlation) requires correlation coefficients of 0.38 and 0.49 for significance at the 95% and 99% levels. The three stippled or cross-hatched areas represent the locations of the equatorial trough in the north Indian Ocean, the equatorial trough north of Australia, and the region of large SST anomalies associated with El Niño.

Figure 3 implies that deficient ISMR is followed by anomalously warm SST in the north Indian Ocean and equatorial east Pacific Ocean, and anomalously cold SST north of Australia. Opposite SST anomalies follow excess ISMR.

The Indian monsoon has been shown to influence north Indian Ocean SST (Joseph and Pillai 1984, 1986; Meehl 1987; Shukla 1987; Rao and Goswamy 1988). Deficient (excess) ISMR warms (cools) the tropical

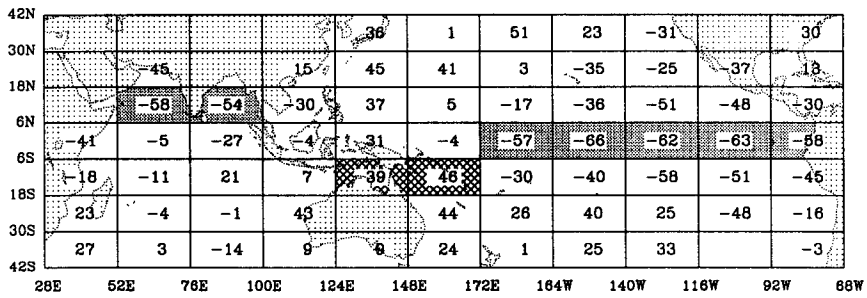

FIG. 3. Correlation coefficient × 100 between ISMR and following SON SST anomaly in each 12° × 24° box for the 27-year period 1957–1983. SST anomaly has been corrected for trend by removing an 11-year running mean. Areas of relevence to this study are stippled or cross hatched (see text).

Indian Ocean, mainly through a weaker (stronger) surface wind field, which affects the SST through weaker (stronger) fields of evaporative fluxes and coastal and open-ocean upwelling (Joseph and Pillai 1986; Krishnamurti 1981). North Indian Ocean SST cools from May to August, unlike other oceans of the Northern Hemisphere during this period. The amplitude of this cooling is controlled by the monsoon's surface wind field and that controls the intensity and sign of the SST anomaly from the end of the monsoon until the following monsoon.

The correlation between the east-central Pacific and ISMR is also well known. Previous studies have shown a connection between ISMR and El Niño (Angell 1981; Rasmusson and Carpenter 1983; Mooley and Parthasarathy 1984b; Parthasarathy and Pant 1985).

It is not known why the SST anomalies north of Australia are correlated with ISMR, but the correlation

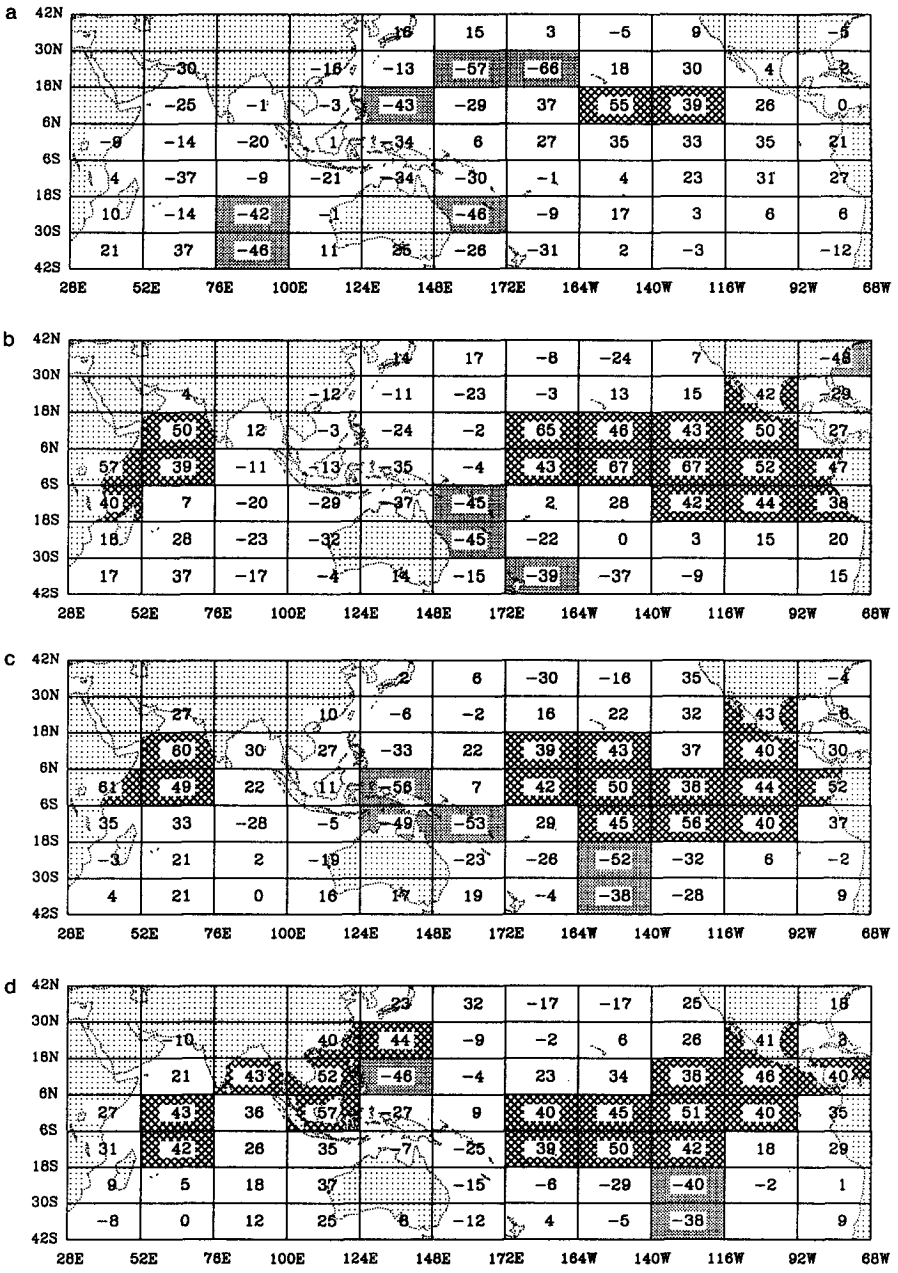

FIG. 4. Correlation coefficient × 100 between the date of ASMO from 1957/58 to 1983/84 and the SST anomaly for (a) preceding MAM season; (b) preceding JJA season; (c) preceding SON season; (d) contemporaneous DJF season. Areas with correlation greater than +0.37 are cross hatched, and areas with correlation less than −0.37 are stippled.

may come through the association between ISMR and El Niño (Rasmusson and Carpenter 1983). The relation between SST anomalies north of Australia and El Niño is shown in composite studies of El Niño (Rasmusson and Carpenter 1982; Nicholls 1984c; Halpert and Ropelewski 1989). During SON one year prior to the mature phase of an El Niño, the waters north of Australia are anomalously warm and those in the eastern Pacific are anomalously cold. The anomalies have opposite signs one year later.

Figure 4 shows the correlation between the date of ASMO and SST for three seasons prior to onset and for the season concurrent with onset. The SON season in Fig. 4c corresponds to Fig. 3. There are marked similarities between the two figures, implying (but not proving) that ISMR and ASMO are linked through SST anomalies. The regions of large correlation in Fig. 3 over the northwestern Indian Ocean, north of Australia, and in the equatorial east-central Pacific all roughly correspond to prominent features on Fig. 4c, but are of opposite sign. The anomaly pattern in the northern Indian Ocean actually becomes established during the June, July, August (JJA) season (Fig. 4b), consistent with the creation of the anomalies by the surface wind field during the Indian monsoon. During the SON and the December, January, February (DJF) seasons (Figs. 4c and 4d) the correlations have expanded throughout the northern Indian Ocean, but have weakened slightly during DJF.

The correlations north of Australia grow until SON (Figs. 4a to 4c) and then drop dramatically during DJF (Fig. 4d). Nicholls (1984b) showed that SST anomalies

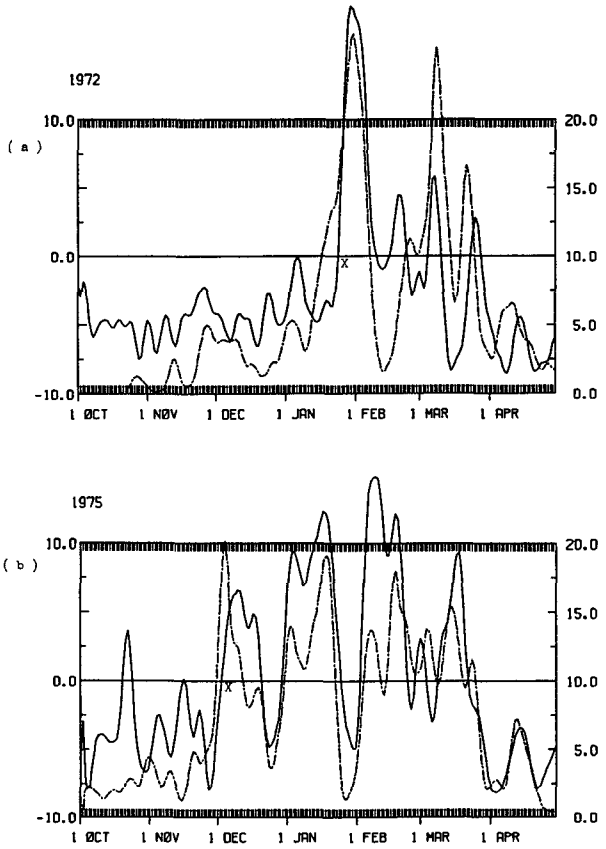

FIG. 5. 850 mb (lightly filtered) daily zonal wind at Darwin (solid line) and area averaged rainfall over northern Australia for October through April (a) 1972/73 and (b) 1975/76. Wind scale is in m s^{-1} (left axis) and rain scale is in mm (right axis). Onset is indicated by an "X."

TABLE 1. Correlations between the SST anomalies of the SON season at areas A, B, and C and those between the SON SST anomalies and the following ASMO for the period 1957–1983. Here, A, B, and C are the stippled or cross hatched areas of the Indian Ocean, the ocean north of Australia, and the equatorial eastern Pacific Ocean, respectively, in Fig. 3.

Correlated pairs	Coefficient of correlation	Coefficient of correlation for significance of 95%	99%
SON SST anomaly at A and ASMO	0.52	0.39	0.50
SON SST anomaly at B and ASMO	−0.54	0.40	0.51
SON SST anomaly at C and ASMO	0.47	0.39	0.50
SON SST anomaly (A–B) and ASMO	0.61	0.39	0.50
SON SST anomalies at A and C	0.68	0.43	0.55
SON SST anomalies at B and C	−0.69	0.38	0.49
SON SST anomalies at A and B	−0.47	0.38	0.49

in this region change sign during DJF. The temporal evolution of the correlation pattern north of Australia suggests that anomalies may have a controlling effect on ASMO since they peak during the season just prior to onset. The correlations in the east-central Pacific, however, peak during JJA (Fig. 4b).

Table 1 illustrates the connection between SON SST anomalies averaged in each of the three shaded regions of Fig. 3 and the ASMO that follows, along with the correlations (corrected for serial correlation) necessary for statistical significance at the 95% and 99% levels. The correlation between the SST of the north Indian Ocean or the ocean north of Australia and ASMO is about the same, while that between the equatorial eastern Pacific and ASMO is slightly smaller. Since the Indian and Australian SSTs are each better correlated with ASMO than with each other, it is not surprising that the difference between these shows a large increase in explained variance when correlated with ASMO.

The multiple correlation of the date of ASMO with the SON SST anomalies of the Indian Ocean and the ocean north of Australia is 0.62. Adding the eastern

Pacific SSTs to the regression does not increase the correlation. The multiple correlations of ASMO with SST anomalies in the eastern Pacific and Australian waters and that with the eastern Pacific and Indian oceans is 0.56 and 0.54, respectively. Thus, it may be inferred that the presence of warm waters in the eastern Pacific is not the controlling factor in the variability of the date of ASMO during the period studied in this paper.

5. Two contrasting cases of ASMO

The ASMO dates used in this study are those derived by Hendon and Liebmann (1990) using the combined wind and rainfall index as described briefly in section 2. In this section we give two examples of the wind and rainfall variations that were used to define ASMO.

a. Monsoon onset in 1972/73

Figure 5a shows the variation in daily 850-mb zonal wind at Darwin (lightly filtered) and the area-averaged daily rainfall over northern Australia in a typical delayed ASMO case. The first day of a spell of wet westerlies is identified as monsoon onset day. ASMO date is 23 January 1973, a delay of 29 days from the normal onset date of 25 December. There were two short but intense spells of active monsoon that season, separated by about 40 days. Holland (1986) noted a mean period of 40 days between active phases of the Australian monsoon. A strong El Niño began early in 1972. There also was a major Indian monsoon drought in 1972, with ISMR of 653 mm, 22.2% below the 30-year mean. During SON 1972, the equatorial trough area of the Indian Ocean had a warm SST anomaly, while the ocean north of Australia had a cold anomaly (Fig. 6a).

b. Monsoon onset in 1975/76

Figure 5b shows the time series of wind and rainfall during 1975/76, a year of early ASMO. The onset occurred on 1 December 1975, 24 days early. During that season's monsoon there were 4 spells of intense monsoon activity, again each separated by about 40 days. A cold event matured in the winter of 1975/76. ISMR in 1975 was 960 mm, 14.4% above the mean. During SON 1975, SST anomalies in the Indian Ocean and the ocean north of Australia were cold and warm, respectively (Fig. 6b), of opposite sign to those during SON 1972.

6. ASMO and Darwin surface pressure

Nicholls et al. (1982) and Nicholls (1984a) have shown an association between the ASMO and the surface pressure at Darwin during the preceding months. The correlation between SON Darwin pressure and the date of ASMO, for the period 1957–1986, is 0.51, significant at the 99% level after correcting for serial correlation.

Shukla and Paolino (1983) have shown that deficient ISMR is followed by a large positive anomaly in Darwin surface pressure lasting several months. The positive pressure tendency at Darwin starts in the Northern Hemisphere winter season prior to a deficient monsoon and continues until the end of the monsoon season

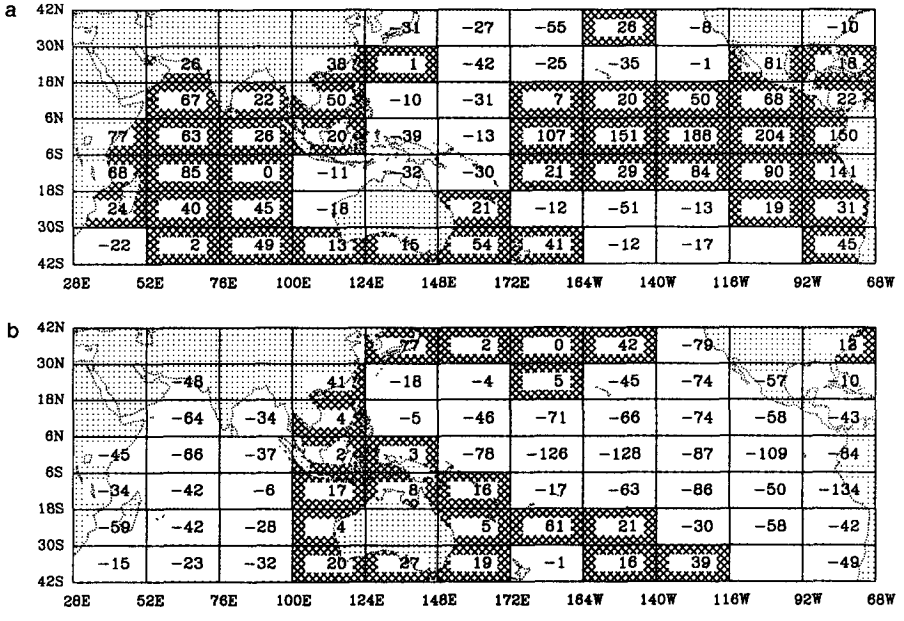

FIG. 6. SST anomalies × 100 (from 11-year running mean) for SON (a) 1972 and (b) 1975. Positive anomalies are cross hatched.

TABLE 2. The change in mean sea level pressure at Darwin, April minus January, in the years of deficient and excess ISMR and in the years of El Nino and cold events. Its long period average for 1939–1984 is 3.0 mb and standard deviation is 1.3 mb.

Deficient monsoons				Excess monsoons			
With El Niño		Without El Niño		With cold event		Without cold event	
Year	Pressure change (mb) (Apr–Jan)	Year	Pressure change (mb) (Apr–Jan)	Year	Pressure change (mb) (Apr–Jan)	Year	Pressure change (mb) (Apr–Jan)
1939	4.4	1968	5.6	1942	1.8	1953	2.0
1941	2.8	1974	4.8	1970	1.8	1956	3.5
1951	4.1	1979	3.7	1973	1.7	1959	2.8
1965	4.9			1975	1.3	1961	1.9
1972	4.8						
Mean pressure change (Mb)	4.2		4.7		1.7		2.5

(Fig. 2 of their paper). Positive (negative) pressure anomaly and pressure tendency are both associated with deficient (excess) ISMR years. They used data of the period 1901–1981, which contained 14 deficient monsoons and 12 excess monsoons. Of the 14 deficient monsoons, only 8 are associated with moderate/strong El Niño (Quinn et al. 1987); of the 12 excess monsoons, only 6 are associated with cold events (Kiladis and Diaz 1989). Shukla and Mooley (1987) listed the values of the change in Darwin pressure from January to April for the period 1939–1986. Nine deficient monsoons have occurred during the common period 1939–1981. Eight excess monsoons have occurred during the same period. The change in January to April Darwin pressure in all these cases, stratified to deficient (excess) monsoons accompanied by El Niño (cold events) or not, are given in Table 2. This shows indirectly the association of the variability of ASMO with that of ISMR.

7. A hypothesis regarding the variability of ASMO

We showed in section 3 that the variability of ASMO is closely tied to that of the preceding ISMR. In sections 4 and 5 we showed that both ISMR and ASMO are associated with SST anomalies of the SON season after ISMR and preceding ASMO.

A schematic of the hypothesized sequence of events leading to a delayed ASMO is presented in Fig. 7; early onset occurs with opposite anomalies. A weak Indian summer monsoon causes positive SST anomalies over the tropical Indian Ocean. These positive SST anomalies in turn delay the seasonal transition of the equatorial trough, which results in a delayed ASMO.

El Niño has a role in ASMO variability in at least two ways. First, since El Niño is associated with deficient ISMR, it is also associated with delayed ASMO. Second, El Niño is associated with anomalously cool waters north of Australia, which can also delay ASMO. Thus, warm SSTs in the eastern Pacific are associated with a delayed ASMO.

A positive pressure tendency at Darwin from January through the northern summer is associated with both El Niño and deficient ISMR. By SON, Darwin has developed a large positive pressure anomaly, which is observed prior to delayed ASMO cases. It is not our intention to show that variability of Darwin pressure and ASMO have a cause and effect relation, but that the two are associated.

Murakami et al. (1986), using OLR data, showed that a delay in ASMO is associated with a delay in the seasonal transition of the equatorial cloudiness maxi-

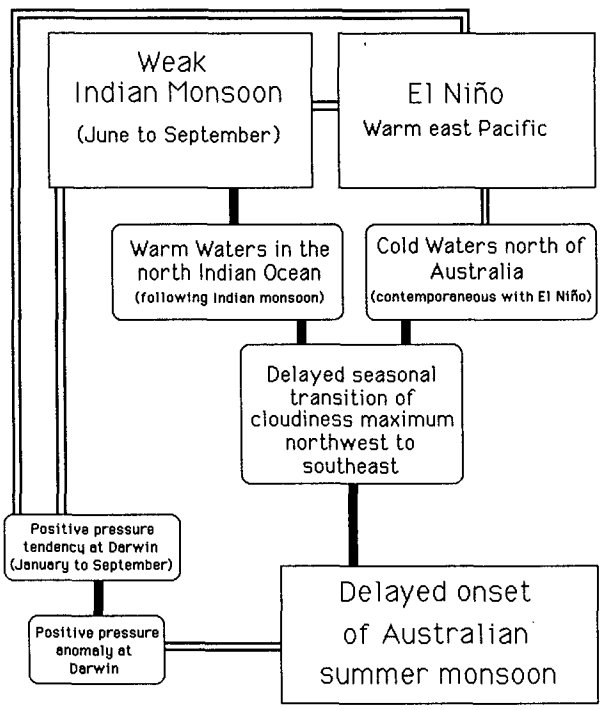

FIG. 7. Schematic of hypothesized sequence of events leading to delayed ASMO. Events (boxes) that have a causal connection (see text) are connected by solid lines. Events (boxes) that occur simultaneously with no causal mechanism implied are connected by double lines.

mum. We show this result directly by compositing cases of delayed and early ASMO for the years during which OLR data are available. Figure 8a is a composite of December OLR for five delayed ASMO cases (1974/75, 1980/81, 1982/83, 1985/86, 1986/87) whose mean date of onset is 9 January. Figure 8b is a similar diagram for five early ASMO cases (1975/76, 1976/77, 1977/78, 1981/82, 1984/85) whose mean date of onset is 5 December.

OLR associated with the delayed ASMO of 1983/84 has been omitted from this composite. The wind and rainfall series used to define onset for this year (similar to Fig. 5) are shown in Fig. 9. An "X" marks the onset as defined by Hendon and Liebmann (1990). The point "Y", about 40 days earlier, shows the requisite increase in wind, but rainfall is slightly short of the required 7.5 mm per day. Had ASMO been defined as occurring during the previous shift to westerlies, it would have been considered an "early" onset (and would have fit the scatter diagram of Fig. 2 almost perfectly). Thus 1983/84 was not included in the composite.

There is a southward and eastward shift of the equatorial cloud band of December between the late ASMO (Fig. 8a) and early ASMO (Fig. 8b) composites. The shift occurs in the direction of the normal seasonal transition of cloudiness as studied by Liebmann and Hartmann (1982) and Meehl (1987) for the northern summer to winter. Thus, the seasonal transition of the cloudiness maximum is later than usual prior to a delayed ASMO.

Figure 8c shows the difference in cloudiness between delayed and early onsets. It is representative of an amplified delayed onset. Excess convection in the western tropical Indian Ocean (denoted by negative OLR differences) and the deficient convection in the ocean north of Australia characterize a delay in ASMO. These are the areas of large positive correlation in the Indian Ocean and negative correlation in the ocean north of Australia in the SON season prior to ASMO (Fig. 4c). Enhanced convection is also evident along the equator east of the date line, characteristic of an El Niño.

It is possible that there is a direct association between SST anomalies in the equatorial eastern Pacific and

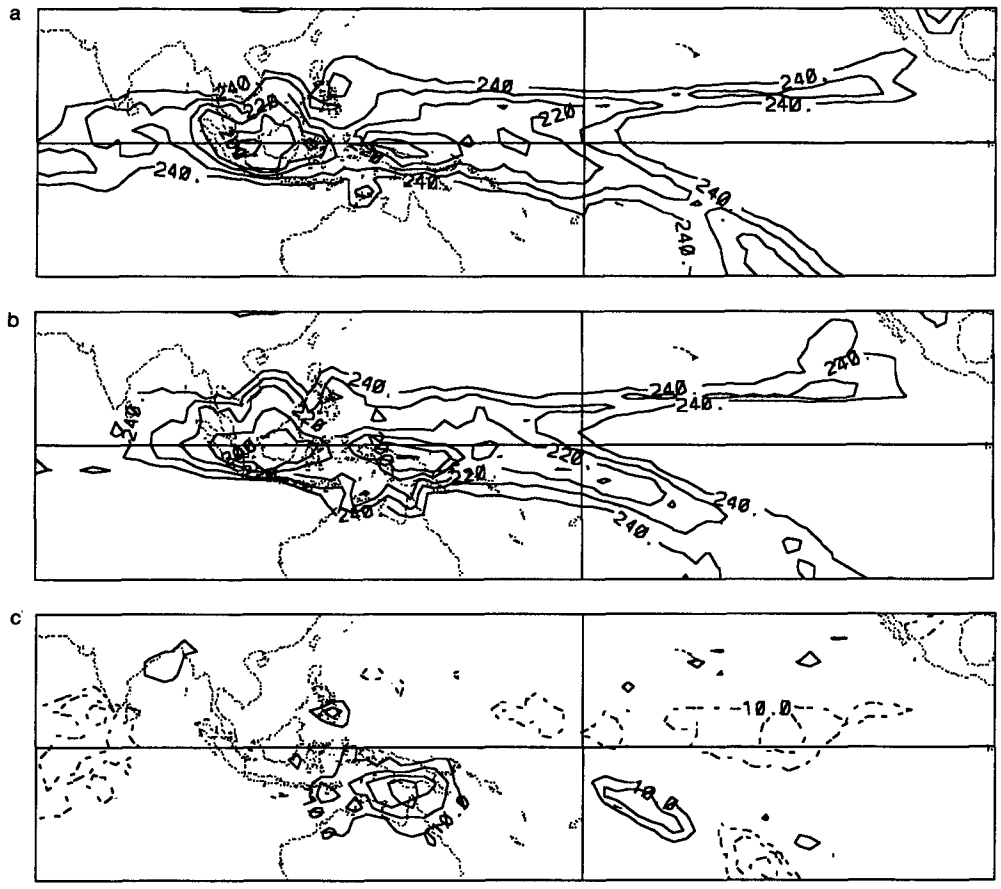

FIG. 8. Composite December OLR for (a) five years with delayed (mean of 9 January) ASMO (see text); (b) five years with early (mean of 5 December) ASMO. Contours decrease from 240 W m^{-2} with an interval of 10 W m^{-2}. (c) Difference (delayed minus early) between (a) and (b). Contour interval is 5 W m^{-2} starting at 10 W m^{-2}. Negative contours are dashed.

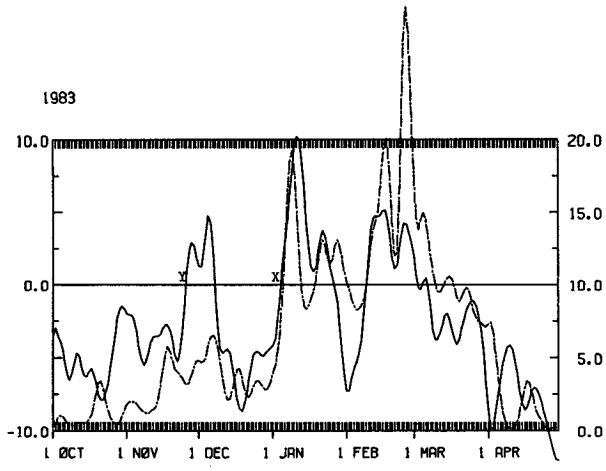

FIG. 9. As in Fig. 5, except for 1983–84. Onset date as defined by Hendon and Liebmann (1990) is marked by "X." The significance of "Y" is discussed in text.

ASMO through changes in the Walker circulation. Figure 8c shows that the convective anomaly near the dateline is as large as the anomaly in the Indian Ocean, although the actual values of OLR are lower over the Indian Ocean than over the eastern Pacific (Figs. 8a and 8b).

A hypothesis similar to the one presented in this paper has been proposed by Joseph (1990) and is supported by data analysis by Joseph and Pyle (1990) to explain the variability of the date of monsoon onset over Kerala in India. According to the hypothesis, monsoon onset takes place there when the SST of the "warm pool" over the Indian Ocean exceeds that of the Pacific warm pool during May to June. Such a situation attracts large-scale moisture convergence to the northern Indian Ocean, in preference to the Pacific warm pool, thus organizing the monsoon onset over India. Most of the cases of delay of monsoon onset are found to be associated with the El Niño warming of the equatorial central Pacific Ocean.

8. Conclusions

We find that deficient ISMR is associated with delayed ASMO and excess ISMR is associated with early ASMO. It is known that deficient ISMR results in warm SST anomalies in the tropical Indian Ocean. We therefore hypothesize that warm Indian Ocean SST anomalies delay the southward and eastward seasonal transition of the equatorial cloudiness maximum during the November to January period, which in turn delays ASMO. Excess ISMR is associated with cold SST anomalies in the Indian Ocean and early ASMO.

Warm and cold events also affect the date of ASMO. Warm events are associated with deficient ISMR, which delays ASMO. Many cases of anomalous ISMR, however, occur in the absence of El Niño/cold events. El Niño (cold events) can also affect ASMO through the cold (warm) SSTs that occur north of Australia during these times. There may also be a direct link between east Pacific SST and ASMO.

ISMR and antecedent SST anomalies both are able to explain about 40% of the variance of the date of ASMO. The 40- to 50-day oscillation (Madden and Julian 1972) also is important for determining the exact date of ASMO. Hendon and Liebmann (1990) showed that ASMO coincides with the arrival of the convective phase of the 40- to 50-day oscillation. Thus, while SSTs control the latitude of the envelope of the 40- to 50-day oscillation, ASMO does not occur until the convective phase of a 40- to 50-day event reaches Australia.

Our finding that a warm SST anomaly in the equatorial Indian Ocean and a cold anomaly in the ocean north of Australia will lead to a delayed southeastward transition of the equatorial trough, we believe, can be easily tested in a general circulation model. Since these models do not produce a realistic 40- to 50-day oscillation, however, it would be difficult to model the resulting variability of ASMO.

Acknowledgments. We wish to thank the following people for their help and suggestions: M. Blackmon, A. Brennan, A. Claerbout, G. Meehl, R. Pyle, and the anonymous reviewers.

REFERENCES

Angell, J. K., 1981: Comparison of the variations in atmospheric quantities with sea surface temperature variations in the equatorial eastern Pacific. *Mon. Wea. Rev.*, **109**, 230–243.

Davidson, N. E., J. L. McBride and B. J. McAvaney, 1983: The onset of the Australian monsoon during winter MONEX: Synoptic aspects. *Mon. Wea. Rev.*, **111**, 496–516.

——, —— and ——, 1984: Divergent circulations during the onset of the 1978–79 Australian monsoon. *Mon. Wea. Rev.*, **112**, 1684–1696.

Fletcher, J. O., R. J. Slutz and S. D. Woodruff, 1983: Towards a comprehensive ocean–atmosphere dataset. *Trop. Ocean–Atmos. Newslett.*, **20**, 13–14.

Gutzler, D. S., and R. A. Madden, 1989: Seasonal variations in the spatial structure of intraseasonal tropical wind fluctuations. *J. Atmos. Sci.*, **46**, 641–660.

Halpert, M. S., and C. F. Ropelewski, 1989: Atlas of tropical sea surface temperature and surface winds. NOAA Atlas No. 8, United States Dept. of Commerce.

Hendon, H. H., and B. Liebmann, 1990: A composite study of onset of the Australian summer monsoon. *J. Atmos. Sci.*, **47**, 2227–2240.

Holland, G. J., 1986: Interannual variability of the Australian summer monsoon at Darwin: 1952–82. *Mon. Wea. Rev.*, **114**, 594–604.

Joseph, P. V., 1990: Warm pool over the Indian Ocean and monsoon onset. *Trop. Ocean–Atmos. Newslett.*, **53**, 1–5.

——, and P. V. Pillai, 1984: Air–sea interaction on a seasonal scale over north Indian Ocean—Part I: Interannual variations of sea surface temperature and Indian summer monsoon rainfall. *Mausam*, **35**, 323–330.

——, and ——, 1986: Air–sea interaction on a seasonal scale over north Indian Ocean—Part II: Monthly mean atmospheric and oceanic parameters during 1972 and 1973. *Mausam*, **37**, 159–168.

——, and R. J. Pyle, 1990: Variability of date of onset of summer monsoon rains over Kerala (India) and its association with El

Niño. *International TOGA Scientific Conference,* Honolulu, Abstracts Publication, WMO, SCOR, IOC & ICSU.

Kiladis, G. N., and H. F. Diaz, 1989: Global climatic anomalies associated with extremes in the Southern Oscillation. *J. Climate,* **2,** 1069–1090.

Krishnamurti, T. N., 1981: Cooling of the Arabian Sea and the onset-vortex during 1979. Recent progress in equatorial oceanography. A report of the final meeting of SCOR working group 47 in Venice, NOVA University, NYIT Press.

Liebmann, B., and D. L. Hartmann, 1982: Interannual variations of outgoing IR associated with tropical circulation changes during 1974–1978. *J. Atmos. Sci.,* **39,** 1153–1162.

Madden, R. A., and P. R. Julian, 1972: Description of global-scale circulation cells in the tropics with a 40–50 day period. *J. Atmos. Sci.,* **29,** 1109–1123.

Meehl, G. A., 1987: The annual cycle and interannual variability in the tropical Pacific and Indian Ocean regions. *Mon. Wea. Rev.,* **115,** 27–50.

Mooley, D. A., and B. Parthasarathy, 1984a: Fluctuations in all India summer monsoon rainfall, 1871–1978. *Clim. Change,* **6,** 287–301.

——, and ——, 1984b: Indian summer monsoon and east equatorial Pacific sea surface temperature. *Atmos.–Ocean,* **22,** 23–35.

Murakami, T., L.-X. Chen and A. Xie, 1986: Relationship among seasonal cycles, low-frequency oscillations, and transient disturbances as revealed from outgoing longwave radiation data. *Mon. Wea. Rev.,* **114,** 1456–1465.

Nicholls, N., 1984a: A system for predicting the onset of the north Australian wet season. *J. Climatol.,* **4,** 425–435.

——, 1984b: The Southern Oscillation, sea surface temperature, and inter-annual fluctuations in Australian tropical cyclone activity. *J. Climatol.,* **4,** 661–670.

——, 1984c: The Southern Oscillation and Indonesian sea surface temperature. *Mon. Wea. Rev.,* **112,** 424–432.

——, and F. Woodcock, 1981: Verification of an empirical long-range weather forecasting technique. *Quart. J. Roy. Meteor. Soc.,* **107,** 973–976.

——, J. L. McBride and R. J. Ormerod, 1982: On predicting the onset of the Australian wet season at Darwin. *Mon. Wea. Rev.,* **110,** 14–17.

Parthasarathy, B., and G. B. Pant, 1985: Seasonal relationships between Indian summer monsoon rainfall and the Southern Oscillation. *J. Climatol.,* **5,** 369–377.

Quenouille, M. H., 1952: *Associated Measurements.* Butterworths Scientific.

Quinn, W. H., V. T. Neal and S. E. Antunez de Mayolo, 1987: El Niño occurrences over the past four and a half centuries. *J. Geophys. Res.,* **92,** 14 449–14 461.

Rao, K. G., and B. N. Goswami, 1988: Interannual variations of sea surface temperature over the Arabian Sea and the Indian monsoon—a new perspective. *Mon. Wea. Rev.,* **116,** 558–568.

Rassmusson, E. M., and T. H. Carpenter, 1982: Variations in tropical sea surface temperature and surface wind fields associated with the Southern Oscillation–El Niño. *Mon. Wea. Rev.,* **110,** 354–384.

——, and ——, 1983: The relationship between eastern equatorial Pacific sea surface temperatures and rainfall over India and Sri Lanka. *Mon. Wea. Rev.,* **111,** 517–528.

Shukla, J., 1987: Interannual variability of monsoons. *Monsoons,* J. S. Fein and P. L. Stephens, Eds., Wiley and Sons, 399–463.

——, and D. Paolino, 1983: The Southern Oscillation and long range forecasting of summer monsoon rainfall over India. *Mon. Wea. Rev.,* **111,** 1830–1837.

——, and D. A. Mooley, 1987: Empirical prediction of the summer monsoon rainfall over India. *Mon. Wea. Rev.,* **115,** 695–703.

Slutz, R. J., S. J. Lubker, J. D. Hiscox, S. D. Woodruff, R. L. Jenne, D. H. Joseph, P. M. Steurer and J. D. Elms, 1985: Comprehensive ocean–atmosphere dataset: Release 1. NOAA Environmental Research Laboratories, Climate Research Program, Boulder, 268 pp. [NTIS PB86-105723.]

Troup, A. J., 1961: Variations in upper tropospheric flow associated with the onset of Australian summer monsoon. *Indian J. Meteorol. Geophys.,* **12,** 217–230.

Wolter, K., S. J. Lubker and S. D. Woodruff, 1989: Trimming—a potential error source in COADS. *Trop. Ocean–Atmos. Newslett.,* **51,** 4–7.

Woodruff, S. D., R. J. Slutz, R. L. Jenne and P. M. Steurer, 1987: A comprehensive ocean–atmosphere dataset. *Bull. Amer. Meteor. Soc.,* **68,** 1239–1250.